Selectivity difference between hydrogenation of acetophenone over CNTs and ACs supported Pd catalysts

Yi-zhi Xiang [1], Yong-an Lv, Tie-yong Xu, Xiao-nian Li [*], Jian-guo Wang [**]

Institute of Industrial Catalysis, Zhejiang University of Technology, State Key Laboratory Breeding Base of Green Chemistry Synthesis Technology, Hangzhou, 310014, PR China

ABSTRACT

Selectivity difference between hydrogenation of acetophenone over carbon nanotubes (CNTs) and commercial activated carbons (ACs) supported Pd catalysts has been investigated. The selectivity of α-phenylethanol over the Pd/CNTs catalyst is significantly higher than that over the Pd/ACs. The optimal yield of α-phenylethanol over the Pd/CNTs catalyst is 94.2% at 333 K under atmospheric H_2 pressure for 255 min, but it is only 47.9% over the Pd/ACs catalyst. HRTEM characterization and density functional theory (DFT) study of the two catalysts suggested that the defects of the carbon support are the main anchoring sites for Pd nanoparticles. Additionally, mechanistic study of the acetophenone hydrogenation over the two catalysts suggested that the different adsorption modes of reaction intermediates (products) on the two kinds carbon supported Pd nanoparticles are responsible for the dramatic selectivity difference.

© 2011 Elsevier B.V. All rights reserved.

1. Introduction

Carbon materials are attractive supports in heterogeneous catalysis because of their specific properties that may be tailored to activity and selectivity [1]. Carbon nanotubes (CNTs), as a kind of novel carbon materials, could be promising supports for catalysts since they own excellent electronic properties, good chemical stability, and large surface areas [2]. Our previous study by density functional theory (DFT) suggested that noble metal nanoparticles adhered on the point defect of CNTs might be acted as a good catalyst in a series of reactions, such as fuel cell and hydrogenation [3]. Additionally, experimental examples on the use of CNTs as catalyst support, such as Pt/CNTs for the hydrogenation of nitrobenzene [4], trans-β-methylstyrene and trans-stilbene [5], 3-methyl-2-butenal [6] and citral [7], Pd/CNTs for the oxidation of benzylic alcohol [8] and Suzuki cross-coupling reactions [9], and bimetallic Pt–Ru/CNTs [10], Pt–Ni/CNTs [11], and Pd–Ru/CNTs [12] for selective hydrogenation of crotonaldehyde and cinnamaldehyde have also been extensively studied. However, there are only few studies have been done on the systematic comparison of the effects of carbon support (CNTs, and traditional activated carbons [ACs]) on the adhesion of noble-metal nanoparticles and their catalytic properties. Although

the influence of the carbon support (multi-walled carbon nanotubes [MWNT], graphite nanofibers [GNF], single-walled carbon nanotubes [SWNT], and commercial activated carbons [ACs]) on the selective hydrogenation of cinnamaldehyde on both monometallic and bimetallic catalysts have been investigated by Serp and coworkers [10], the comparison between CNTs and ACs supports in terms of the hydrogenation mechanism and result catalytic performance is still lack.

The selective hydrogenation of acetophenone to α-phenylethanol is of great importance in the synthesis of pharmaceuticals and fragrances [13,14]. Generally, the hydrogenation of acetophenone was carried out by using transition metals, such as Ni, Pt, Ru, Pd and Cu [15–23] supported on Al_2O_3, ACs, TiO_2, SiO_2 and zeolites etc. as the catalysts. However, the high selectivity for the hydrogenation of the carbonyl group is frequently not easy to achieve due to the formation of unwanted products ethylbenzene via side reactions, such as the hydrogenolysis of α-phenylethanol.

In this study, we observed that the CNTs supported Pd catalyst (Pd/CNTs) is highly selective for the hydrogenation of acetophenone into α-phenylethanol, which is particularly notable since the selectivity of α-phenylethanol is significantly lower on the commercial activated carbon supported Pd catalyst (Pd/ACs). The influence of the carbon supports (CNTs and ACs) on the adhesion of Pd nanoparticles and the catalytic properties in the hydrogenation of acetophenone were investigated by means of DFT calculations. Additionally, the characteristics of the two catalysts were studied by means of X-ray diffraction (XRD), transmission electron microscopy (TEM), CO chemisorption, and N_2 physical adsorption

(BET). The possible mechanistic reasons for the selectivity difference of the two carbon supported Pd catalyst were also discussed.

2. Experimental

2.1. Catalysts

CNTs were supplied by Prof. W. Fei from Tsinghua University, and ACs was purchased from Shaowu Xinsen Chemical Industry Co. Ltd. The Pd/CNTs and Pd/ACs catalysts were prepared by adding an aqueous solution of H_2PdCl_4 ($0.05\,g_{metal}\,ml^{-1}$) into an aqueous slurry of the carbon support (CNTs or ACs without oxidative pretreatment, the ratio of support to water was 1 g:10 mL) to obtain a Pd nominal loading of 3 wt%. The slurry was vigorously stirred at room temperature for 2 h, then the pH values was adjusted to 8–10 by adding an aqueous solution of sodium hydroxide (10 wt.%) dropwisely. Finally, the slurry was washed by distilled water until the pH = 7 before dried under vacuum at 383 K for 10 h.

The morphology and Pd particle size distribution of the Pd/CNTs and Pd/ACs catalysts were determined by a Tecnai G2 F30 S-Twin TEM at an operating voltage of 300 kV. The BET surface areas of the Pd/CNTs and Pd/ACs catalysts were determined by nitrogen physical adsorption–desorption at 77 K under vacuum condition using a NOVA 1000 e surface area analyzer (Quantachrome Instruments Corp.). The dispersion of Pd particle on the CNTs and ACs support were also measured by CO uptake through a pulse chemisorption method with a mass spectrometry (Omnistar^{TM}) at ambient temperature and pressure.

2.2. Acetophenone hydrogenation

The hydrogenation of acetophenone was carried out at 333 K in a 50 mL flask. The Pd/CNTs or Pd/ACs catalyst (0.1 g) was reduced in situ in the flask at 333 K for 2 h with H_2 (10 mL min^{-1}) before the catalytic tests (the catalyst will be ignited when it was contacted with air after reduction, which means the Pd has been reduced). Then acetophenone 1 mL and ethanol 20 mL ($C_{Acetophenone}$ = 0.428 mol/L) was added together into the flask. During the reaction, H_2 (10 mL min^{-1}) was bubbled through the liquid phase (To study the catalytic mechanism, H_2 will be switched into N_2 at the same flow rate at a certain reaction time, or the Pd/CNTs catalyst will be replaced by ACs after the reaction. See Fig. 4 for the experimental setup); the liquid was stirring extensively with a magnetic stirrer. The products were analyzed by a GC–MS (Agilent 6890GC-5973MS equipped with a 25 m-HP-5 capillary column with MS detector).

The recycling performance of the Pd/CNTs catalyst was also conducted in the same flask under identical conditions without separation and reactivation of the catalyst. After the first use of the catalyst, another 1 mL acetophenone was added directly to the liquid without any separation (noted as cycle 1), or the liquid in the flask was carefully removed by a pipette (after setting for at least 30 min) and replaced by another 1 mL acetophenone and 20 mL ethanol (noted as cycle 2). Reactions were then carried out under the identical conditions as mentioned before.

The acetophenone hydrogenation rates over the Pd/CNTs and Pd/ACs were calculated based on the conversion data shown in Fig. 3. The first three data were selected for calculation, because the conversion is lower at this initial stage, which make sure that the hydrogenation rate could not be affected by the changes of acetophenone concentration (the conversion of acetophenone is increased linearly). The equations for the calculation of the hydrogenation rate (r (mol/g$_{cat}$/min)) is shown below,

$$r = -\frac{dn_A}{dt} \times \frac{1}{m_{cat}},$$

$$n_A = n_{A0} \times (1 - x),$$

In which n_A represent the molar amount of acetophenone in the reactor, t represent the reaction time, m_{cat} represent the amount of catalyst, n_{A0} represent the initial amount of acetophenone added into the reactor (0.00856 mol), x represent the conversion. Because the conversion of acetophenone was initially increased linearly, the hydrogenation rate can now be expressed as

$$r = n_{A0} \times \text{slope of } x \times \frac{1}{m_{cat}},$$

The turnover frequency (TOF) of the Pd/CNTs and Pd/ACs catalysts for the hydrogenation of acetophenone were calculated based on the CO chemisorption results.

2.3. DFT calculation

The first-principles DFT calculations were performed using the DMol^3 module in Materials Studio [24,25]. The generalized gradient approximation (GGA) with PW91 functional [26] is used to describe the exchange-correlation (XC) effects. The double numerical plus polarization (DNP) basis set are used in expanded electronic wave functional. In this study, the periodic supercells of (5, 5) CNTs were adopted with optimized length of a, b, and c lattices of 25.00, 20.00, and 9.76 Å. The length of c is four times of that in the periodicity of (5, 5) CNTs. The minimum distance between opposing sidewalls of neighboring CNTs is bigger than 9.30 Å, which can avoid interaction among repeating supercells. The activated carbons are modeled by the two layers graphite (0001) slab in 4 × 8 unit cell. The Brillouin zone is sampled by 1 × 1 × 2 k and 2 × 1 × 1 k points using the Monkhorst–Pack scheme for CNTs and ACs. All of atoms were fully relaxation during the geometry optimization. For all of the calculations, the convergence in energy and force was set to 10^{-5} eV and 2×10^{-3} eV/Å.

3. Results and discussion

3.1. Pd/ACs and Pd/CNTs catalysts

The nitrogen physical adsorption results of the Pd/CNTs and Pd/ACs catalysts show that the BET surface areas of the two catalysts are 218.5 and 1659 m^2 g^{-1}, respectively (Table 1). The corresponding pore volume and pore diameter are 1.61 cc g^{-1} and 14.7 nm, and 1.12 cc g^{-1} and 1.35 nm, respectively. These results suggest that the Pd/ACs catalyst shows a significantly higher BET surface area than the Pd/CNTs, but the Pd/CNTs catalyst possess the higher pore volume and radius than the Pd/ACs.

The reprehensive TEM micrograph of the Pd/CNTs and Pd/ACs catalysts are shown in Fig. 1. The carbon nanotubes are curved, twisted together and display an average external diameter ranging between 8 and 40 nm. All of the Pd nanoparticles supported on the CNTs are round-shaped, but it seems that the shape of the Pd nanoparticles on ACs is amorphous. The reprehensive HRTEM images of the Pd/CNTs catalyst are shown in Fig. 1(b) and (c). The lattice spacing of the Pd particle (Fig. 1(b)) is 0.228 nm, consistent with the interplanar distance of the Pd (1 1 1) plane. To note that XRD analysis, due to small particle size and low metallic loading of Pd, do not gives reliable indications on these crystallographic aspects. Although the Pd nanoparticle size of the Pd/ACs catalyst is quite similar with that of Pd/CNTs from the TEM images, the dispersion of Pd on the CNTs and ACs are 21.4 and 39.6%, respectively, according to the CO chemisorption (Table 1). Additionally, it must be noted that the Pd nanoparticles of the Pd/ACs catalysts are also present predominantly on the interface and boundary of the two layer of the ACs.

Table 1
Physicochemical property of the Pd/CNTs and Pd/ACs catalysts and the hydrogenation activity.

Catalyst	Surface area ($m^2 g^{-1}$)	Pore volume ($ml\,g^{-1}$)	Pore radius (nm)	CO uptake ($ml\,g^{-1}$)	Pd dispersion (%)[a]	Hydrogenation rate ($mol\,g_{cat}^{-1}\,min^{-1}$)	TOF (min^{-1})
Pd/CNTs	218.5	1.61	14.7	1.35	21.4	0.0185	307
Pd/ACs	1659	1.12	1.35	2.5	39.6	0.0500	448

[a] Calculated from CO chemisorption.

3.2. The adhesion of Pd clusters on ACs and CNTs

In order to provide the insights of the adhesion mechanism of Pd clusters on the CNTs and ACs, a series of Pd clusters on the pristine and point defected (with carbon vacancy) CNTs and ACs have been investigated by means of DFT calculations. Fig. 2 shows the geometries and binding energies of the most stable Pd clusters on CNTs and ACs. The favorable binding site of Pd_1 on both CNTs and ACs is the bridge site of carbon atoms, in which the average Pd–C distance is 2.12 and 2.18 Å. The binding energy is 2.00 and 1.93 eV, which reveals Pd have very similar adhesion properties with Pt on the carbon materials [3]. The structure of the most stable Pd_4 and Pd_7 cluster on both CNTs and ACs are very similar and the Pd atoms in the first layer are more than those in the second layer. On the point defected CNTs and ACs, Pd clusters are always located on the vacancies. And the binding energies are nearly 3 times than those on the pristine ones. Therefore, it can be expected that the defects are the main anchoring sites of metal clusters (for example Pd in this study) on the carbon materials. In fact, the defects are also including the steps, bending, boundary, interface and kinks of CNTs and ACs as can be seen from HRTEM micrographs shown in Fig. 1.

3.3. Selective hydrogenation of acetophenone

The experimental results of the selective hydrogenation of acetophenone over the Pd/ACs and Pd/CNTs catalysts are shown in Fig. 3. As shown in Fig. 3A, the conversion of acetophenone is increased from 20 to 95% with the increases of reaction time from 10 to 120 min (carried out at 333 K over the Pd/ACs catalyst), but the selectivity of α-phenylethanol is decreased from 71 to 25%, accordingly, and the selectivity is further decreased to only 3.8% when the reaction time prolonged to 150 min (the only by-product observed is ethylbenzene). These results suggested that the α-phenylethanol can be further hydrogenated into ethylbenzene over the Pd/ACs catalyst.

The hydrogenation of acetophenone over the Pd/CNTs catalyst is quite different from that over the Pd/ACs catalyst under the identical conditions, as can be seen from Fig. 3B. The conversion of acetophenone and selectivity of α-phenylethanol are 95.3 and 96.5%, respectively, when the reaction was carried out over the Pd/CNTs catalyst at 333 K for 240 min. Additionally, the selectivity of α-phenylethanol is only slightly decreased from 96.5 to 95.8%, when the reaction time is further prolonged from 240 to 255 min (the conversion of acetophenone is increased from 95.3 to 98.3%). These results suggested that the hydrogenalysis
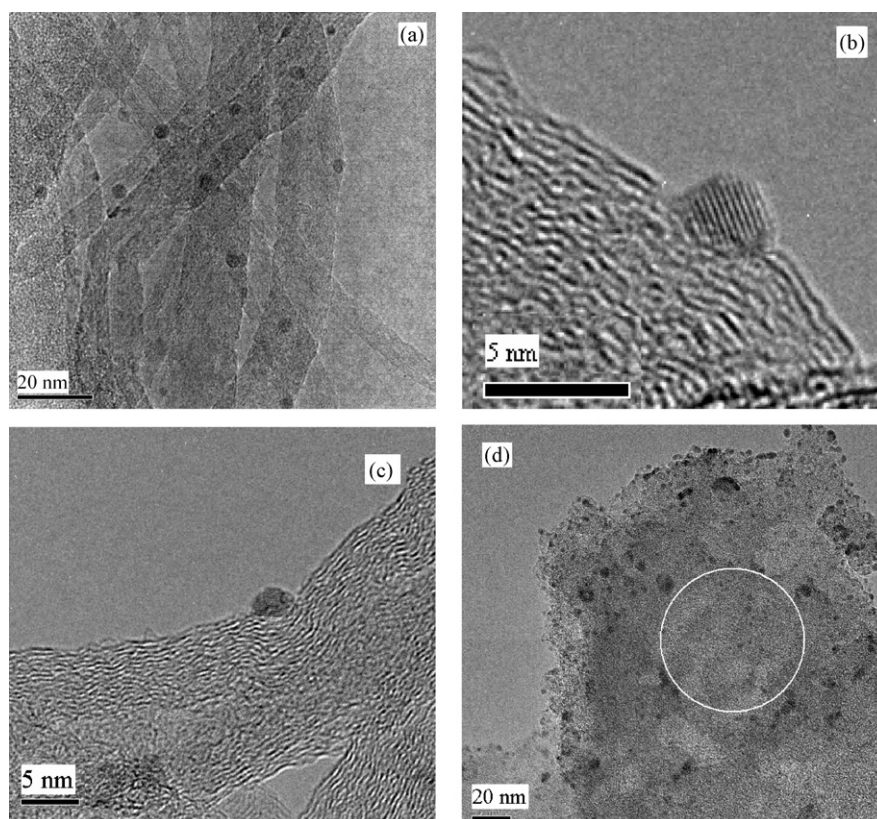

Fig. 1. Reprehensive TEM and HRTEM micrographs of the Pd/CNTs and Pd/ACs catalysts. (a), (b) and (c) Pd/CNTs, and (d) Pd/ACs.
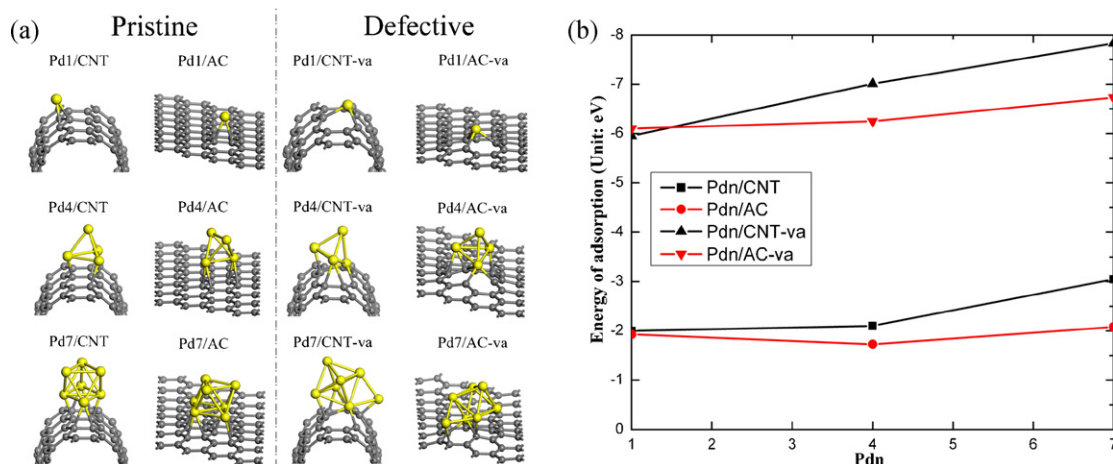
Fig. 2. (a) Optmized structures (b) Binding energies of Pdn (n = 1, 4, 7) on the outer-side wall of pristine and point defected CNTs and ACs.

of α-phenylethanol into ethylbenzene is highly inhibited over the Pd/CNTs catalyst.

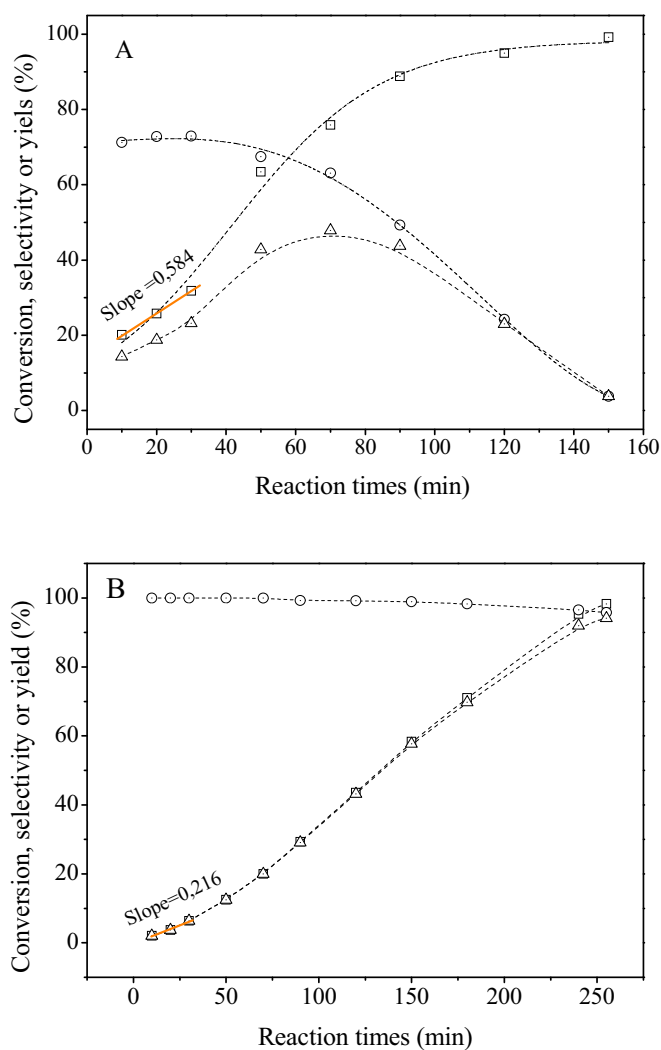Compared the catalytic performance of the two carbon supported Pd catalysts for the hydrogenation of acetophenone, we can conclude that the Pd/CNTs catalyst shows significantly higher selectivity for α-phenylethanol than the Pd/ACs catalyst, although the activity of the Pd/ACs catalyst is slightly higher than the Pd/CNTs catalyst, the hydrogenation rate and TOF over the Pd/CNTs and Pd/ACs are 0.0185 $mol\,g_{cat}^{-1}\,min^{-1}$ and 307 min^{-1}, and 0.05 $mol\,g_{cat}^{-1}\,min^{-1}$ and 448 min^{-1}, respectively, as shown in Table 1. The optimal yields of α-phenylethanol over the Pd/ACs and Pd/CNTs catalysts are 47.9 and 94.2%, respectively.

It must be pointed out that the recycling performance of the Pd/CNTs is not so good without reactivation since the acetophenone conversion decreased from 96% (for the fresh catalyst) to 80% (for the second use cycle 1), but to 52% (for the second use cycle 2). These results suggested that trace amounts of impurities in the solvent (ethanol) and material (acetophenone) will result in the deactivation of the Pd/CNTs catalysts. Reactivation of the recycled Pd/CNTs catalyst by washing, drying (desorption) or reduction to remove the adsorbed impurities is generally required to realize the recycling of the catalyst.

3.4. Acetophenone hydrogenation mechanism

In order to analyze the reason of the selectivity difference between the hydrogenation of acetophenone over the Pd/CNTs and Pd/ACs catalysts, the acetophenone hydrogenation mechanism over the two catalysts was discussed. There are two possible routes for the formation of by-product ethylbenzene, i.e. (1) hydrogenalysis of α-phenylethanol and (2) dehydration of α-phenylethanol
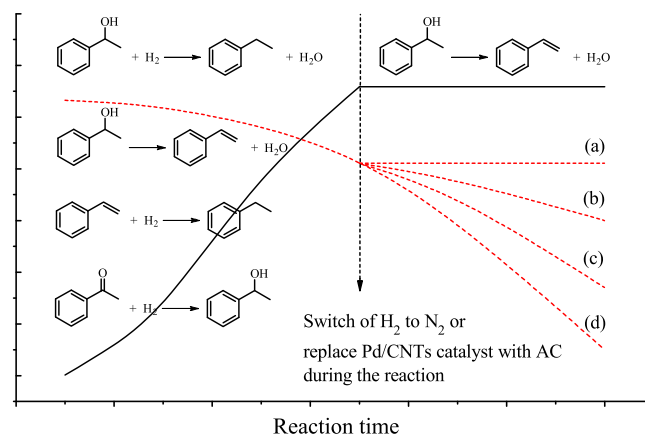

Fig. 3. Experimental results of the selective hydrogenation of acetophenone for α-phenylethanol over (A) Pd/ACs catalyst and (B) Pd/CNTs catalyst. (□) Conversion, (○) α-phenylethanol selectivity and (△) α-phenylethanol yield.

Fig. 4. Scheme of the experimental setup on the mechanistic study by switching H₂ to N₂ or replace Pd/CNTs catalyst with ACs during the reaction. (solid line) acetophenone conversion, (dash line) α-phenylethanol selectivity.
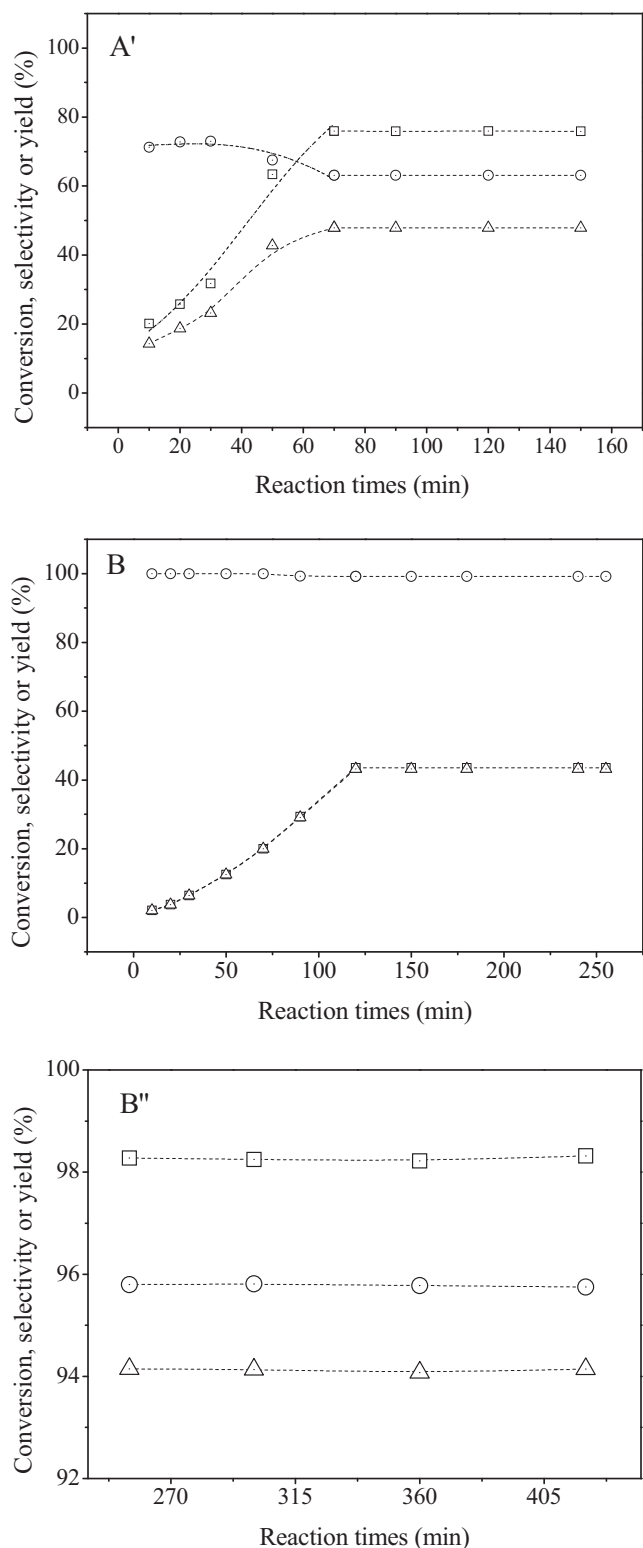
Fig. 6. Optimized structures of α-phenylethanol on Pd7/CNTs and Pd/ACs with vacancy.

α-phenylethanol selectivity by switching H_2 to N_2 or replacing of Pd/CNTs catalyst by ACs during the reaction. The switch of H_2 to N_2 or replace of Pd/CNTs catalyst by ACs during the reaction, will result in the stop of the hydrogenation of acetophenone and hydrogenalysis of α-phenylethanol (reactions with H_2), but the selectivity of α-phenylethanol will be still decreased if the α-phenylethanol was dehydrated into styrene with the prolonged reaction time. Therefore, the position of the selectivity line in Fig. 4(dash line) after switch of H_2 to N_2 or replace of Pd/CNTs catalyst by ACs could represent the ratio of the occurrence of route (1) and (2), i.e., lines (a), (b) and (c), and (d) represents the occurrence of only route (1), both routes (1) and (2), and only route (2), respectively, as shown in Fig. 4.

Fig. 5 shows the experimental results of the hydrogenation of acetophenone according to the reaction scheme shown in Fig. 4 by switching H_2 to N_2 or replacing Pd/CNTs by ACs. As shown in Figs. 5A and B, all of the reactions was ceased as soon as H_2 was switched to N_2, because the products distribution was no longer changed when the reaction was carried out under N_2 atmospheric. Additionally, the replacement of the Pd/CNTs catalyst by ACs, after the reaction was carried out for 250 min, no reaction was observed either, even through under H_2 atmospheric (Fig. 5B″). The selectivity of α-phenylethanol was not decreased means that by-product ethylbenzene could only be formed in the presence of H_2 and Pd metallic active site. Additionally, ethylbenzene was produced through the direct hydrogenalysis of α-phenylethanol or acetophenone, while the dehydration of α-phenylethanol followed by hydrogenation of styrene could not be the real mechanism for the formation of ethylbenzene.

With this information, we further investigated the adsorption properties of α-phenylethanol on the Pd/CNTs and Pd/ACs catalysts, respectively, by means of DFT calculations, to reveal the difference on the hydrogenation of acetophenone over these two catalysts. The optimized geometries of α-phenylethanol on Pd7/CNTs and Pd7/ACs are shown in Fig. 6. The results suggested that the adsorption configurations of α-phenylethanol are different. On Pd7/CNTs, the benzene ring of α-phenylethanol is directly bonded with Pd clusters, while the hydroxyl-group is far away from the support

Fig. 5. Experimental results of the hydrogenation of acetophenone (A′) switch of H_2 to N_2 at 70 min over Pd/ACs catalyst, (B′) switch of H_2 to N_2 at 120 min over Pd/CNTs catalyst, (B″) replace of Pd/CNTs catalyst with ACs at 250 min under H_2 atmospheric. (□) conversion, (○) α-phenylethanol selectivity and (△) α-phenylethanol yield.

into styrene and followed by hydrogenation of styrene. For the second route, α-phenylethanol should be dehydrated into styrene in the absence of H_2 over the Pd/ACs, or in the presence of H_2 over the ACs. In order to determine the reaction route to form the by-product ethylbenzene, we can monitor the changes of
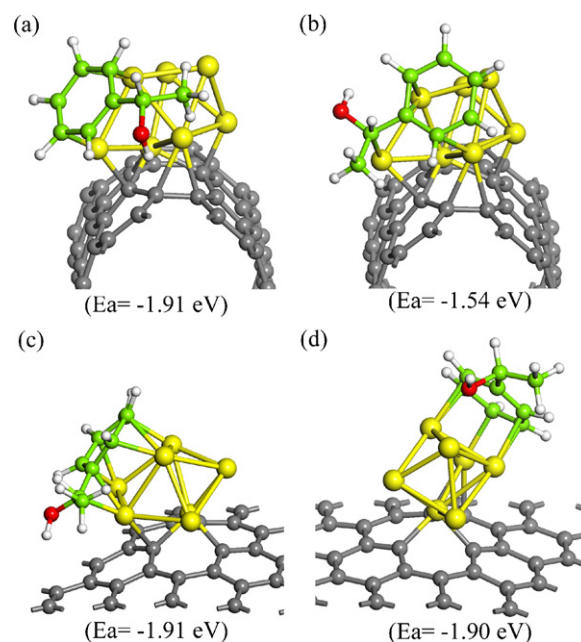
and the Pd clusters, in which the shortest distance between oxygen and Pd is 2.81 Å. On Pd7/ACs, although the benzene ring of α-phenylethanol is bonded with Pd cluster, the hydroxyl-group in α-phenylethanol is close to the interface of Pd clusters and ACs support, in which the distance between oxygen in hydroxyl and Pd is 2.38 Å. Therefore, the hydrogenation of acetophenone on the Pd/ACs catalyst result in the hydrogenolysis of the hydroxyl-group in α-phenylethanol molecular, which will result in the formation of by-product ethylbenzene. While, the hydrogenolysis of the hydroxyl-group in α-phenylethanol molecular could be inhibited because the hydroxyl-group in α-phenylethanol is far away from the interface of the Pd particle and CNTs support when α-phenyl ethanol was adsorbed on the Pd/CNTs catalyst. These could be the reason for the significantly difference in the α-phenyl ethanol selectivity over the two catalyst.

4. Conclusions

The catalytic hydrogenation of acetophenone over the Pd/CNTs catalyst shows significantly higher α-phenylethanol selectivity than that over the Pd/ACs catalyst, the optimal yields over the two catalysts are 94.2 and 47.9%, respectively. TEM characterization of the two catalysts suggested that the defects, including the steps, bending, boundary, interface and kinks of CNTs and ACs, are the mainly anchoring sites of the Pd particles, and the results from DFT calculation also proved that the Pd particles incline to adsorb on the point defect rather than the smooth part of the CNTs and ACs. The mechanistic study of the acetophenone hydrogenation over the two catalysts suggested that by-product ethylbenzene was produced only through the hydrogenolysis of α-phenylethanol. On the Pd/CNTs catalyst, the hydrogenolysis is inhibited, because the hydroxyl-group in α-phenylethanol is far away from the support and the Pd clusters (the shortest distance between oxygen and Pd is 2.81 Å). However, the Pd/ACs catalyst favors the occurrence of hydrogenolysis due to the hydroxyl-group is close to the interface of Pd clusters and ACs support (the distance between oxygen in hydroxyl and Pd is 2.38 Å). These different adsorption modes of α-phenylethanol on the two kinds of catalysts are responsible for the dramatic selectivity difference.

References

[1] E. Auer, A. Freund, J. Pietsch, T. Tacke, Appl. Catal. A: Gen. 173 (1998) 259–271.
[2] P. Serp, M. Corrias, P. Kalck, Appl. Catal. A: Gen. 253 (2003) 337–358.
[3] J.G. Wang, Y.A. Lv, X.N. Li, M.D. Dong, J. Phys. Chem. C 113 (2009) 890–893.
[4] C.H. Lia, Z.X. Yua, K.F. Yao, S.F. Ji, J. Liang, J. Mol. Catal. A Chem. 226 (2005) 101–105.
[5] T. Onoe, S. Iwamoto, M. Inoue, Catal. Commun. 8 (2007) 701–706.
[6] V. Lordi, N. Yao, J. Wei, Chem. Mater. 13 (2001) 733–737.
[7] F. Qin, W. Shen, C.C. Wang, H.L. Xu, Catal. Commun. 9 (2008) 2095–2098.
[8] A. Villa, D. Wang, N. Dimitratos, D.S. Su, V. Trevisan, L. Prati, Catal. Today 150 (2010) 8–15.
[9] X.C. Chen, Y.Q. Hou, H. Wang, Y. Cao, J.H. He, J. Phys. Chem. C 112 (2008) 8172–8176.
[10] H. Vu, F. Gonçalves, R. Philippe, E. Lamouroux, M. Corrias, Y. Kihn, D. Plee, P. Kalck, P. Serp, J. Catal. 240 (2006) 18–22.
[11] Y. Li, C.H. Ge, J. Zhao, R.X. Zhou, Catal. Lett. 126 (2008) 280–285.
[12] J.S. Qiua, H.Z. Zhang, X.N. Wang, H.M. Han, C.H. Liang, C. Li, React Kinet. Catal. Lett. 88 (2006) 269–275.
[13] K. Bauer, D. Garbe, Ullmann's Encyclopedia, vol. A11, 3rd ed., VCH, New York, 1988, p. 141.
[14] P. Rylander, Hydrogenation Methods, Academic Press Inc., London, 1985, p. 66.
[15] G.F. Santori, A.G. Moglioni, V. Vetere, G.Y. Moltrasio Iglesias, M.L. Casella, O.A. Ferretti, Appl. Catal. A: Gen. 269 (2004) 215–223.
[16] C. Chen, H. Chen, W. Cheng, Appl. Catal. A: Gen. 248 (2003) 117–128.
[17] L. Cerveny, Z. Belohlav, M.N.H. Hamed, Res. Chem. Intermed. 22 (1996) 15–22.
[18] M. Casagrande, L. Storaro, A. Talon, M. Lenarda, R. Frattini, E. odriguez-Castellon, P. Maire-les-Torres, J. Mol. Catal. A: Chem. 188 (2002) 133–139.
[19] M.A. Aramendia, V. Borau, J.F. Gomez, A. Herrera, C. Jimenez, J.M. Marinas, J. Catal. 140 (1993) 335–343.
[20] A. Drelinkiewicza, A. Waksmundzka, W. Makowski, J.W. Sobczak, A. Krol, A. Zieba, Catal. Lett. 94 (2004) 143–156.
[21] M. Bejblova, P. Zamostny, L. Cerveny, J. Cejka, Collect. Czech. Chem. Commun. 68 (2003) 1969–1984.
[22] J.M. Bonnier, J.P. Damon, J. Masson, Appl. Catal. 42 (1988) 285–297.
[23] J. Masson, S. Vidal, P. Cividino, P. Fouilloux, J. Court, Appl. Catal. A Gen. 99 (1993) 147–159.
[24] B.J. Delley, Chem. Phys. 92 (1990) 508–517.
[25] B.J. Delley, Chem. Phys. 113 (2000) 7756–7764.
[26] J.P. Perdew, Y. Wang, Phys. Rev. B 45 (1992) 13244–13249.